

GRAVITY INVESTIGATION OF THE MANSON IMPACT STRUCTURE, IOWA

J. B. Plescia<sup>1</sup>

MS 183-S01

Earth and Space Sciences Division

Jet Propulsion laboratory

California Institute of Technology

Pasadena, CA 91109

Submitted: July 15, 1994

Revised: November 22, 1994

(1994)  
(11)

<sup>1</sup>present address: NASA Headquarters, Code SLC, Washington, DC 20546

Geological Society of America Special Paper

## ABSTRACT

X A gravity survey of the Manson impact structure, Iowa, reveals a residual gravity anomaly associated with the structure. A pronounced gravity high occurs over the central uplift and an annular gravity low surrounds the high. Total gravity relief is of the order 7-9 mGal. Numerous anomalies observed in the residual field reflect variations in the density of the basement complex. Aeromagnetic anomalies over the region show no correlation with the structural components of the impact feature; presumably they reflect lithologic variations in the crystalline basement. The Manson impact structure has a diameter of ~36 km and a central peak diameter of ~10 km. Structural uplift of the Proterozoic crystalline surface amounts to 3-4 km. Modeling of the structure indicates a central uplift composed of crystalline basement rocks surrounded by an annulus of breccia and disturbed country rock which extends to depths of 3 km, which has a density contrast of  $-0.13 \text{ g cm}^{-3}$ . The complex gravity anomaly of the central uplift shows that it is not a simple plug like body, but has a more complex shape - perhaps an incipient central ring or pitted peak.

## INTRODUCTION

The Manson impact structure is located in northwestern Iowa (center at 42°34,44' N; 94°33.60' W; Fig. 1). The structure had been known as a geologic anomaly for at least 60 years (Norton and others 1912; Norton, 1928) on the basis of water well data showing the presence of crystalline basement at shallow depth (below the glacial till) in a region where the typical depth to crystalline basement is 4000-6000 m (Anderson and Hartung, 1992). Manson is an ~ 36 km diameter structure having the classic form for a complex impact crater, a central uplift (composed of uplifted Proterozoic crystalline bedrock), surrounded by a "moat" filled with impact breccia and melt, and a terraced rim (composed of Proterozoic and Paleozoic country rocks) that have slumped into the crater along concentric faults. Manson is the largest confirmed impact structure in the United States.

Over the last several years, an extensive, multidisciplinary study has been conducted of the Manson impact to better understand its structure and age (Shoemaker and others, 1993). Hartung and Anderson (1988) present a compilation of the data on the Manson impact structure prior to this recent activity. The results of much of the current phase of research are presented in this volume. In order to better understand the diameter and the details of the internal structure of the Manson impact, a gravity survey was undertaken to extend and augment the data base of Holtzman. The results of that work are presented here,

French (1984) suggested that the Manson structure might be the source of shock-metamorphosed quartz in the Cretaceous-Tertiary boundary clay in

eastern Montana and hence that it might be the Cretaceous-Tertiary boundary crater. Recent  $^{40}\text{Ar}/^{39}\text{Ar}$  analyses by Izett and others (1993) of sanidine from the impact melt material recovered from the M-1 drill hole indicate an age of 73.8~ 0.31 Ma for Manson; thus, this age is inconsistent with a Cretaceous-Tertiary boundary age. However, the crater remains an important site for understanding the effects of the cratering process on the Earth's crust, cratering dynamics, for constraining the terrestrial cratering rate, and possibly the effects of large impacts on the Earth's climate,

## REGIONAL GEOLOGY

The Manson structure has been significantly eroded and is buried beneath a regional blanket of glacial till. None of the rocks of the structure crop out and the subsurface geology is based on drill hole and seismic data (Anderson and Hartung, 1992).

The general undisturbed stratigraphic section (Figs. 2 a, b) of the area includes Quaternary sediments, Mesozoic, Paleozoic, and Middle Proterozoic sedimentary rocks overlying Early Proterozoic plutonic and metamorphic basement rocks. Basement rocks include gneiss of the Penokean volcanic belt (1.86- 1.80 Ga) intruded by Middle Proterozoic anorogenic granites (1.50- 1.43 Ga) both of which are cut by diabase dikes (1.0 Ga). Regional subsidence occurred about 1.0 Ga associated with the formation of the Midcontinent Rift System and a thick section of sedimentary rocks was laid down. The sedimentary section includes the "Red Clastics" - red shales, siltstones, and sandstones formed in a fluvial environment. Above the Red Clastics is a Middle Cambrian section consisting of multiple marine transgressive-regressive

cycles of carbonates, shales, siltstones and sandstones with minor continental sediments. In turn, Jurassic Ft. Dodge beds (shale, sandstone, and siltstone), sandstone dominated Cretaceous Dakota Formation, and Graneros shale, Greenhorn limestone, and Carlisle shales constitute the remainder of the preserved stratigraphic section. The youngest unit of the region is a 30 - 90 m thick layer of Quaternary glacial till.

Regional basement geologic features have a northeasterly trend. In the Manson area this is expressed by a southeastward thickening of the sedimentary units and the northeast-trending Mid-continent rift which follow the older Archean trends. Initially, an extensional environment existed with the formation of graben and horsts of the Mid-continent rift system. Later compressional stresses resulted in uplift and the formation of the Iowa Horst (Fig. 2b) along the Northern Boundary Fault Zone. The Precambrian crystalline surface is offset by approximately 6-8 km across this fault.

#### PREVIOUS GRAVITY WORK

Holtzman (1970) originally conducted a gravity survey of the area. However, his data extended out to a radius of only ~5 km beyond the dimensions of the structure as they were understood at the time. When the earlier survey was conducted, the "disturbed zone" was assumed to be elliptical with the long axis oriented north-south; a north-south diameter of 32 km and an east-west diameter of 29 km. Subsequent work has shown the structure to be circular having a diameter of ~36 km. Thus, Holtzman's data ended just inside the rim of the structure as the structure is presently understood,

As a result of his study, Holtzman concluded that the outer boundary of the Manson structure could not be delineated on the basis of the gravity data, that a negative anomaly is associated with the crater and caused by the low-density brecciated sedimentary rocks, and that the other anomalies were the result of density variations in the basement or elastic rocks. Sharpton and Grieve (1990) modeled the gravity data of Holtzman and concluded that the central uplift had a density of  $\sim 2.44 \text{ g cm}^{-3}$  and was surrounded by an annular lens of breccia having a density of  $\sim 2.30 \text{ g cm}^{-3}$ . They estimated the maximum thickness of the breccia as  $\sim 3 \text{ km}$ . Further, they felt that two high-density ( $2.80 \text{ g cm}^{-3}$ ) bodies at shallow depth were required to model the gravity and attributed these to possible vestiges of the impact melt sheet.

#### DATA COLLECTION AND REDUCTION

Gravity data coverage now extends for 65 km east-west and 63 km north-south over the structure (Fig. 3). Measurements were made at every section corner resulting in data points every 1.6 km (1 mile) over the structure and for at least 5 km beyond the edge as defined by the seismic reflection profiles (see below). Over the central portion of the structure, stations were collected at 800 m (0.5 mile) intervals along roads at 1/4 section corners. Beyond 5 km from the rim and extending to the edge of the survey, data were collected about every 3 km (2 miles) at section corners. The total number of data points used in this analysis exceeds 1100.

Station location and elevation were obtained from the U. S. Geological Survey 7.5' topographic map sheets. The original elevations of Holtzman (1970) were determined from barometric surveys and were estimated to be accurate to

± 1.2 m. in this analysis, Holtzman's observed gravity values were used; however, the elevations were corrected using elevations from the 7.5' map sheets. The base station at the Fort Dodge airport used by Holtzman could not be located; apparently it has been destroyed by later construction. Absolute gravity for this survey, allowing the two data sets to be merged, was provided by reoccupying a number of stations from the original survey.

Data were reduced using the U.S. Geological Survey Bouguer program which includes latitude, free air, Bouguer, and curvature corrections. The data have not been corrected for terrain effects as this correction was trivial given the relatively flat surface; relief within tens of meters of the station was typically a less than 1 meter. Bouguer corrections were made using a density of  $2.57 \text{ g cm}^{-3}$ . The resulting gravity values were then gridded and contoured to prepare map presentations of the data. A grid composed of  $50 \times 50$  elements (grid point spacing of 1.3 km) was used for contouring. Grid point values were determined by an inverse distance weighting method using the eight nearest data points.

## RESULTS

### *Simple Bouguer Gravity*

The regional Bouguer gravity field is illustrated in Fig. 4a and 4b. Figure 4a is a contour map of the field with a contour interval of 2.0 mGal; Fig. 4b is a three-dimensional (3D) representation of the gridded Bouguer gravity. The field is characterized by an asymmetric northeast-trending gravity trough; gravity gradients on the west side being less than on the east ( $\sim 2.2 \text{ mGal km}^{-1}$

vs.  $2.8 \text{ mGal km}^{-1}$ ). Locally, gradients exceed  $5 \text{ mGal km}^{-1}$  in the easternmost areas. Values are about  $-64 \text{ mGal}$  in the northwest and decrease to about  $-7 \text{ mGal}$  before rising up to as high as  $+20 \text{ mGal}$  in the southeasternmost corner of the study area; total gravity relief is of the order of  $100 \text{ mGal}$ . In the northwestern corner the gravity field is fairly flat. A northwest-trending low cuts across the western flank of the gravity trough at the location of the Manson structure.

To first order, the Bouguer gravity field can be understood in the context of the geology of the Precambrian basement (geologic context is taken from Anderson, 1986 a, b; Figs. 2 a, b). The gravity high at the southeast corner of the survey area is associated with the mid-continent gravity high; which extends across the Midwest from the Lake Superior area southwest into Kansas, Thiel (1956) originally correlated the gravity high with Keweenaw volcanic rocks and gabbro exposed in northern Minnesota and Wisconsin. The adjacent northeast-trending gravity low is caused by a basin containing low-density elastic sediments shed from the rocks associated with the Mid-continent gravity high. These flanking lows correlate with Precambrian feldspathic sandstone also exposed farther north in Minnesota and Wisconsin.

Modeling of a simple basin and adjacent ridge reproduces much of the observed Bouguer gravity signature. The large gradient in the southeast corner of the map is associated directly with the "Northern Boundary Fault" which marks the western edge of the Iowa Horst. The density contrast associated with the fault results from the Thor Igneous Complex to the southeast juxtaposed against the Red Clastics to the west. The general decrease in gravity southeastward is the result of a thickening section of Cambrian and



younger strata. A distinct gravity signature associated with the Manson impact is not apparent in the Bouguer map (Fig. 4 a, b). A closed high at "A" is coincident with the southwestern side of the central peak, but other aspects of the Manson structure are not defined by the gravity field.

### *Residual Bouguer Gravity*

Because the Bouguer gravity is dominated by the high-amplitude long-wavelength features, the subtle small-scale anomalies that may be associated with specific structural elements of the Manson impact are difficult to resolve. Therefore, the effects of the long-wavelength gravity must be removed. To identify the small-scale anomalies that would correlate with specific structural elements, the residual gravity from the structure must be isolated. A series of polynomial surfaces were fit to the Bouguer gravity field and the residual values contoured. These polynomial surfaces represent the long-wavelength component of the gravity field, i.e., the regional gravity. The residual gravity obtained after subtracting the polynomial surface would correspond to the local anomalies associated with the structure of the impact.

After analysis of several different order polynomials, a 5th-order polynomial surface and residuals were chosen for illustration. This version seems to remove most of the regional effects while retaining several small-scale anomalies. Although a polynomial of sufficient order could be calculated to remove all the short-wavelength features, it would effectively remove all of the signal of the structure. Therefore, a balance had to be struck between preservation of the signature due to the structure and the acceptance of some anomalies unrelated to the structure.

X

Figures 5a and 5b illustrate the 5th-order polynomial surface in contour form and in a 31° perspective. The basement geology, as noted above, is dominated by only a few major structures; the Iowa horst, the Boundary Fault, and the southeastward thickening section of the Red Clastics. Therefore, the 5th-order trend surface is a good approximation of the regional gravity; the 5th-order residuals thus reflect the more localized aspects of the crustal structure.

Many positive and negative gravity anomalies are apparent in the residual gravity field (Fig. 6). The central uplift of the crater ("A") is characterized by two positive anomalies having amplitudes of about +4 mGal separated by a gentle northwest-trending saddle located approximately at the crater center. Surrounding the central high is a ring of gravity lows of variable amplitude (-2 to -4 mGal). These lows surround the central high although the minimum value of the gravity anomaly varies. Beyond this annular low, several positive anomalies separated by significant lows occur. Gravity highs are elongated in an easterly direction in areas north and west of the structure; elsewhere at greater distance, the highs have northeast or northerly trends. To first order, these anomalies do not exhibit a pattern obviously associated with an impact crater. Typically one might expect a gravity high associated with the central uplift (if the central uplift exposes relatively dense rock), surrounded by an annular low (resulting from low-density impact breccia and fill), possibly surrounded by more complicated gravity signatures resulting from the terracing and uplifted rim. However, this is not the pattern observed at Manson, which suggests that many of these anomalies are the result of density contrasts in the basement rocks. Their

isolated nature, steep gradients, and relatively short wavelengths are also consistent with variations in the basement density.

X Correlations of the specific anomalies with bedrock geology is not simple. The central positive gravity anomaly "A" (Fig. 6) at the central uplift of the crater corresponds to the crystalline basement occurring at a shallow depth. The paired anomalies suggest that the central uplift does not have the simple shape of a plug. Based on the dimensions of the gravity anomalies, the central uplift has a diameter of ~ 10 km. (correlations with lithologies of the crystalline basement are difficult because of the absence of exposure. Lithologic maps of the basement (e.g., Fig. 2 a, b from Anderson, 1986a) are based on scattered well data. Thus, the actual extent of any single basement lithology may be better defined by the gravity data. In addition to the limited data provided by wells, the crystalline basement is buried beneath the Red Clastics in the southeastern portion of the study area preventing penetration by walk.

At the northern margin, the low at "B" may be caused by an occurrence of the Central Iowa Arch Granite, most of the known extent of which lies north of the survey area. The elongate low at "C" may correlate with granites and rhyolites of the Eastern Granite-Rhyolite Interval. The high in the northwest corner "D" would correspond then to the (amp Quest gneiss. The southeastern area is covered by the Red Clastics which occur in the Duncan and Defiance Basins. Anomalies in these areas have larger half-widths and lower gradients suggesting a deeper source perhaps in the crystalline basement. They may reflect density variations either in the crystalline rocks or the Red Clastics. To the southeast, the area of significant gravity gradient with northeast-

trending isogals corresponds to the Northern Boundary Fault. The large gradients result from the significant density contrast across the fault.

## REFLECTION PROFILE

A seismic reflection profile (fig. 7) along an east-west road extending from the central uplift to the eastern margin of the Manson impact structure (Anderson and Hartung, 1992) was run by the Amoco company in the mid 1970s. These reflection data define the major structural elements of the impact. The profile extends a total length of 29 km, beginning ~ 3 km west of the center of the uplift and extending a total of 12 km east beyond the rim.

Within the Manson impact structure, three major structural elements of the crater are observed; the central uplift (extending to a radius of 5 km); the crater moat (5 to 10 km radius), and the terraced rim (10 km to 16 km). The central uplift is characterized by uplifted crystalline basement locally covered with impact breccia. The crater moat is filled with disrupted strata, both impact and fall back breccia as well as breccia formed by material slumping off the rim and the central uplift. A thin layer of horizontal, undisturbed strata overlies the ejecta material, apparently postdating the cratering event. The terraced rim shows a number of blocks which are displaced along inward dipping listric normal faults. The down-dropped blocks are composed of tilted Paleozoic strata and the underlying Red Clastics and locally completely overturned, as indicated by drill hole data. The extent of penetration of the faults into the crystalline basement is unclear. At the eastern end, outside the structure, the reflection profile shows ~750 m of flat-lying Paleozoic rocks, principally carbonate and sediments overlying a series of east-dipping

reflectors. The east-dipping reflectors are interpreted to be the southeastward thickening wedge of the Red Clastics. Finally, the crystalline basement is detected only at depths of 4800 m at the eastern end; the crystalline basement shallows to the west,

Detailed gravity profiles were run along the east-west seismic reflection profile line as well as along a north-south line through the center of the structure to attempt to determine the extent to which structural details in the seismic reflection profile can be resolved. Readings were made at 800 m (0.5 mile) intervals along these profiles. For illustration, the simple Bouguer gravity, residual gravity and seismic reflection profile for the east-west line are illustrated in Figure 7. This profile provides a simpler picture of the gravity field than the contour maps and indicates a high degree of correlation with the major structural components.

The simple Bouguer gravity (light dashed line; Fig. 7) shows a broad low reaching a minimum over the zone of "crater ejects" east of the central uplift. Additionally, a slight positive anomaly is observed centered over the eastern half of the central uplift. In order to clearly resolve the anomalies associated with the structure observed in the reflection profile, a residual gravity profile was prepared. Here, a third-order polynomial was fit to the data and the residuals plotted. Because only a one-dimensional profile is being considered, a third-order polynomial was sufficient to remove the regional trend. The residual profile (dark line) shows a significant high (+ 3 mGal) centered over the eastern side of the central uplift; westward over the uplift the gravity decreases to about + 1 mGal, but remains high. This lower gravity to the west of the high corresponds to the area of the gravity saddle illustrated in the

contour map in Figure 6. A gravity low reaching -4 mGal is centered over the "crater ejecta" zone. Farther east the gravity rises, with some irregularity, to a value of about +2 mGal at the edge of the structure.

A positive anomaly characterizes the central uplift reflecting the presence of relatively high-density basement rocks at shallow depth.

However, this anomaly is not a simple circular high. Rather the complex shape reflects the presence of impact breccia locally deposited on the western side of the central uplift and a varied basement lithology within the uplift producing a complex density distribution. The gravity low east of the uplift over the "crater ejecta" can be attributed to the presence of a thick lens of the low-density breccia and disturbed rock extending to several kilometers depth. The depth of the gravity low is not uniform around the central uplift suggesting that the thickness and bulk density of this material varies around the crater. Over the terraced terrane, the complicated gravity apparently reflects faulting and the juxtaposition of different rock types. Based on the gravity profile and the seismic reflection data, the Manson impact structure has a radius of ~18 km.

#### GRAVITY MODELING AND DENSITY DETERMINATIONS

In order to better understand the structure of the Manson impact and the density distribution of the material, the gravity along the east-west reflection profile was modeled. The model is constrained by the features observed in the seismic reflection profile and the densities determined from the core samples and taken from the literature.

### *Density Determinations*

Density determinations were made for material recovered in two of the drill holes, M 1 and M2A (see Anderson, this volume, for a complete description of these cores). Both holes are located on the central uplift (M1 in the northeast corner; M2A in the southeast corner). Density determinations were made on large sections of core to provide bulk rock density estimates in order to avoid the effects of small-scale lithologic variations. Sections of core up to 65 cm long were weighed and measured. The lithified nature of the breccias allowed for longer pieces of intact core to be used; the less lithified sediments required the use of smaller samples, typically 2-25 cm in length. All determinations were made with dry samples. Water saturation, as would occur in situ, would increase the density.

Core M1 is composed of breccia and melt rock overlain by about 50 m of glacial till. From about 50 to 105 m below the surface, the core is composed of suevite, dominated by clasts of predominately Cretaceous sedimentary rocks; between depths of 105 and 150 m the material is an impact melt breccia dominated by clasts of Proterozoic crystalline rocks. Below the impact melt breccia a second interval of suevite occurs from 150 to 200 m. The lowest 25 m of the core is composed of a fragmental breccia. Figure 8 illustrates the calculated dry densities plotted as a function of depth. The density of the breccia ranges from 2.0 to 2.8 g cm<sup>-3</sup> and varies with depth. Variations with depth are significant and appear to reflect layering within the breccia with the transitions between layers being of the order 25 m. The suevite has an average density of  $2.34 \pm 0.30$  g cm<sup>-3</sup>; the impact melt breccia has a density of

$2.53 \pm 0.12 \text{ g cm}^{-3}$ , and the fragmental breccia has an average density of  $2.11 \pm 0.11 \text{ g cm}^{-3}$ .

Densities for lithic clasts from the core were also determined. Banded gneiss and mafic igneous rocks from the crystalline basement have densities of  $2.69 \pm 0.14 \text{ g cm}^{-3}$ ; fragments of Paleozoic limestone had densities of  $2.68 \pm 0.15 \text{ g cm}^{-3}$ . Sediments from the upper part of core M2A were also examined. The sandstones had a density of  $2.10 \pm 0.09 \text{ g cm}^{-3}$  and the shales had a density of  $1.80 \pm 0.08 \text{ g cm}^{-3}$ . These results, however, are only preliminary. Samples of suevite and breccia have been examined from only a single core and the extent to which variation occurs throughout the breccia both with depth and across the crater has yet to be determined. Core M1 penetrated <200 m of a possible 3 km of crater ejects and disrupted rock. Thus, only the shallowest of samples are available for analysis,

Density determinations by other investigators (Thiel, 1956; Coons and others, 1967; Holtzman, 1970; Gupta and others, 1984) for typical mid-continent rocks indicate similar densities; Keweenawan volcanic rocks and gabbro ( $2.90 \text{ g cm}^{-3}$ ); Precambrian crystalline rocks ( $2.7 \text{ g cm}^{-3}$ ); dense basaltic rocks of the Mid-continent gravity high ( $3.0 \text{ g cm}^{-3}$ ); elastic sediments ( $2.30 - 2.40 \text{ g cm}^{-3}$ ), shales ( $2.4 - 2.5 \text{ g cm}^{-3}$ ), limestones ( $2.6 - 2.8 \text{ g cm}^{-3}$ ), and sandstones ( $2.5 \text{ g cm}^{-3}$ ); and glacial deposits ( $2.2 \text{ g cm}^{-3}$ ). Ernstson and Pohl (1974) present logged bulk formation density for the breccia at the Ries structure in Germany. Those data show a considerable scatter in density and an increase in density with depth. Between 300 and 600 m the density increases from about  $2.2 \text{ g cm}^{-3}$  to  $2.6 \text{ g cm}^{-3}$ ; below 600 m the density averages  $\sim 2.65 \text{ g cm}^{-3}$ . The densities from the



upper part of the Rics breccia are consistent with the values derived from core M1 under water saturated conditions.

The densities of the breccia correlate with the magnetic susceptibility. Izett and others (1993) determined magnetic susceptibility of core M1; typical values range from  $10^{-5}$  to  $10^{-3}$  (cgs-v). Susceptibilities peak between about 120 and 140 m below the surface within the impact melt breccia. Below about 150 m within the Suevite, the susceptibility gradually increases with depth and exhibits some scatter. This trend is similar to that observed in the density data. The correlation between density and magnetic susceptibility suggests that the two properties share a similar source. The variations could be due to changes in the mafic matrix material, the amount of lithic fragments, or a secondary, highly magnetic phase which has filled the original porosity thereby increasing the density and the susceptibility.

### *2 1/2 D Gravity Model*

A 2 1/2 D gravity model of the structure was constructed along the line of the reflection profile from the center of the Manson impact structure eastward beyond the rim. The model assumes infinite extent of the bodies perpendicular to the profile. To first order, the dimensions of the bodies were based on the structure derived from the reflection profile; the initial densities used were based on those measured here and those taken from the literature. The gravity profile used in the model is the 3rd-order residual profile derived from the Bouguer gravity (Fig. 7).

The model which best matches the observed gravity is illustrated in Figure 9. It is composed of the crystalline basement complex ( $2.71 \text{ g cm}^{-3}$ ), the Red Clastic wedge ( $2.69 \text{ g cm}^{-3}$ ), Paleozoic section ( $2.75 \text{ g cm}^{-3}$ ), Tertiary sediments within the crater ( $2.59 \text{ g cm}^{-3}$ ), impact breccia and disrupted rock filling a large triangular shaped zone inside the crater and draped over the western portion of the central uplift ( $2.48$  to  $2.57 \text{ g cm}^{-3}$ ), and an overlying layer of glacial till ( $2.20 \text{ g cm}^{-3}$ ). An arbitrary body with a negative density contrast was inserted at the eastern end of the profile to accommodate the decrease in the gravity at the eastern end of the profile. Since individual model bodies have uniform density, this arbitrary body probably represents density variations within the Red Clastics or a different lower density lithology in the crystalline basement,

The fit of the calculated gravity to the residual gravity is generally good. The two important aspects of the model are the central uplift of crystalline rock and the wedge of disturbed low-density rock surrounding the uplift. A density contrast of  $-0.13 \text{ g cm}^{-3}$  between the crystalline rock and the breccia is used in the model. This value is 5-10% lower than the difference between the measured densities of the crystalline rocks and the breccia ( $-0.25 \text{ g cm}^{-3}$  to  $-0.43 \text{ g cm}^{-3}$ ), indicating that the overall density for the breccia in the crater is greater than the samples would indicate. The higher density could be the result of water saturation or increased density with depth due either to compaction, alteration, or increased lithic fragment content,

## COMPARISON OF GRAVITY AND MAGNETIC FIELD DATA

The regional magnetic field of the area around the Manson impact structure (Fig. 10) has been determined by a series of aeromagnetic surveys (Zietz and others, 1976; Henderson, and Vargo, 1965; U. S. Geological Survey, 1976). Aeromagnetic data were collected for the region around Manson along east-west flight lines spaced 1.6 km (1 mile) apart and flown at an altitude of 305m (1000 feet) above ground level and contoured at intervals of 20 and 100  $\gamma$  (1  $\gamma$  = 1 nT). The regional field has a relatively simple character to the southeast of Manson and a more complicated pattern to the northwest; a line trending northeast approximately west of Manson separates these two regions. To the southeast, the field is characterized by northeast-trending contours defining a series of broad northeast-trending magnetic highs and lows. These broad features correlate with the Mid-continent gravity high. To the northwest of Manson, the character is rather different. There the field is dominated by numerous positive magnetic anomalies, typically circular although some are elongate in various directions. These anomalies have widths of 10 km and relief of 1000 to 1500 nT. The difference in magnetic character between the two regions can easily be interpreted in light of the basement geology and the high magnetic susceptibility of the Proterozoic crystalline rocks. To the southeast of Manson the Proterozoic crystalline basement deepens and the Paleozoic sedimentary section thickens; thus the source of the magnetic anomalies is deeper and the field is dominated by the large-scale structure of the Mid-continent gravity high. Northwest of Manson, the Paleozoic cover is absent and the crystalline rocks are at a shallow depth producing high-amplitude anomalies. Thus, the compositional differences of the shallow subsurface are readily reflected in the magnetic field map.

Several magnetic anomalies are geographically associated with the Manson impact, about six positive magnetic anomalies and two negative anomalies occur. These anomalies are -10 km long and 2-3 km wide; magnetic relief is -1000- 1500 nT. Several additional, smaller, highs and lows occur around the region. There is, however, effectively no correlation between the magnetic anomalies within the crater and the three major elements of the crater: the central uplift, the crater moat, and the terraced rim.

The central uplift, where crystalline basement is brought up through the Paleozoic section and buried only by glacial till, is not characterized by a well-defined positive anomaly. Rather a linear positive anomaly extends to the southeast, an elongate positive anomaly occurs on the southwest margin, and a slight negative anomaly characterizes the western part of the central uplift. Positive and negative anomalies occur in both the crater moat and the terraced rim with varying orientations and amplitudes. In neither of these areas do the anomalies take the shape of a feature concentric about the central uplift. This lack of correlation suggests that the magnetic anomalies are not a simple reflection of the near-surface crustal structure of the impact crater. The two magnetic highs associated with the central uplift have steep gradients and short half-widths suggesting they have shallow sources. Most likely, these anomalies result from highly magnetic components of the breccia or crystalline basement rocks. Elsewhere the anomalies have similar steep gradients and short half-widths and must have a shallow source.

The low degree of coincidence between the magnetic and gravity anomalies suggests that the magnetic and density character of the crystalline

basement rocks do not necessarily correlate. In some cases highly magnetic basement rocks do not appear to have high densities; and vice versa. In some instances the density and magnetic character correlate very well. Given the diversity of rock types within the crystalline basement such a lack of correlation is not unexpected. Although there appears to be a correlation in the density and magnetic susceptibility of the impact breccia, at least in core M-1 the contrasts with the surrounding rock are not of such magnitude that a well defined gravity or magnetic anomaly characterizes the crater moat.

## DISCUSSION

The Manson impact structure, 36 km diameter, is a typical complex crater having a central uplift and terraced rim. The gravity signature of Manson impact is also typical of a complex crater with a central positive anomaly and a surrounding annular low. The gravity model presented here and that of Sharpton and Grieve (1990) differ in only a few aspects. Sharpton and Grieve used a density contrast of  $0.14 \text{ g cm}^{-3}$  between the rocks of the central uplift and the surrounding annulus, whereas this model uses  $0.13 \text{ g cm}^{-3}$ . The absolute densities used in the models were quite different, but it is only the relative density that is important. The most significant difference between the models lies in the incorporation of two high-density bodies (interpreted as fragments of the melt sheet) in the Sharpton and Grieve model. Such bodies were not necessary in the model presented in Figure 9. The irregularity in the gravity profile along the terraced rim is probably due to the presence of faulted blocks.

The data suggest that the central uplift at Manson is about 10 km in diameter. Such a diameter is consistent with that for other complex craters (Grieve, 1991). The amount of structural uplift (SU) of the deepest material within the central uplift would amount to about 3 km, based on the relation ( $SU = 0.06 D^{1.1}$ , where  $D$  is the diameter, from Grieve and others, 1981). This value is consistent with the seismic reflection profile.

Anderson and Hartung (1992) interpreted the "crater ejects" as extending to depths of 2-3 km based on the seismic reflection profile. Grieve (1991) suggests that the depth of excavation for complex craters, though not well understood, could be of the order of  $0.13D$ , where  $D$  is the diameter (based on studies from the Decaturville and Steinheim structures). Using this relation, the depth of excavation at Manson would be of the order 5 km, consistent with the interpretations of Anderson and Hartung (1992) and the gravity model presented here. Data from the Siljan structure in Sweden (Dyrelius, 1988), which has a diameter of 55 km, indicates that anomalously low-densities persist to depths of 5 km. The greater density of the modeled wedge thus reflects increasing density with depth, the effect of water saturation, and the inclusion of shattered and disturbed autochthonous country rock below the transient cavity.

Holtzman (1970) suggested that the gravity anomalies and steep gradients to the north and west of the structure were the result of an arcuate fault which juxtaposed shales (presumably filling the crater) with crystalline rocks outside the crater. However, these gradients appear to be caused by density contrasts within the crystalline basement. No gravity signature appears to be associated with the rim of the impact structure. The seismic

reflection profile shows flat lying strata outside the rim and strata dropped down along faults inside the rim. 'There is no indication of uplift around the edge of the structure that might produce a positive anomaly.

X A number of craters have dimensions similar to Manson, such as Azuara Spain and Carswell, Clearwater Lake West, and Slate Islands in Canada, and Siljan Sweden. These craters all exhibit pronounced gravity anomalies in range of -10 to -15 mGal. Figure 11 indicates the gravity anomaly for Manson compared with that for numerous other structures using data taken from Pilkington and Grieve (1992). The Manson impact structure has a total gravity relief (from the central uplift high to the annular low) of the order 7-9 mGal.

The Manson impact structure has a typical, though smaller gravity signature than similar size craters elsewhere. The smaller gravity anomaly with respect to other features indicates a smaller density anomaly among the rocks present at the site. This could be the result of either a smaller volume of disturbed rock or a smaller density contrast. Pilkington and Grieve (1992) cite typical density contrasts of 0.15 to 0.24 g cm<sup>-3</sup> with a mean value of 0.18 g cm<sup>-3</sup> between fractured and undisturbed rocks at several terrestrial impact craters. That value is greater than the contrast of 0.13 g cm<sup>-3</sup> derived from the modeling here by some 10-50%. The difference may result from the breccia and disturbed rocks at Manson having less porosity, greater lithic content, or perhaps having experienced greater compaction than at other impact sites.

## CONCLUSIONS

The Bouguer gravity data show that the Manson impact structure exhibits a well-defined positive anomaly associated with the central uplift and an annular low surrounding the central high. These anomalies are best interpreted to be caused by the presence at a shallow depth of high-density crystalline basement surrounding by low-density breccia, melt rock, and disturbed country rock. Total gravity relief is of the order 7-9 mGal, although the total does depend upon the choice of regional field. The central high is composed of uplifted Proterozoic crystalline rock having densities of  $2.7 \text{ g cm}^{-3}$ ; the surrounding lows are the result of the breccia and melt rock (density  $2.48\text{-}2.47 \text{ g cm}^{-3}$ ).

Modeling of the structure indicates the central uplift is surrounded by a low density material having a density contrast of  $0.13 \text{ g cm}^{-3}$ . Manson impact structure has a diameter of  $\sim 36 \text{ km}$  and a central peak diameter of  $\sim 10 \text{ km}$ . The complex gravity anomaly of the central uplift shows that it is not a simple plug like body, but has a more complex shape - perhaps an incipient central ring or pitted peak. The amplitude of the anomalies on the southeast side is less than the amplitude of the anomalies to the northwest. When viewed in the context of an increase in the depth of the Proterozoic crystalline basement to the southeast, it suggests that the anomalies may be due to variations in the density of the basement rocks rather than the crater itself. No correlation is observed between the aeromagnetic anomalies and the structural components of the impact (central uplift, crater moat, and terraced rim). Presumably the anomalies reflect variations in the magnetic character of the crystalline basement complex.



## ACKNOWLEDGMENTS

This work benefited from discussions with many members of the Manson Study Group. Reviews and comments from Seppo Ilkko, Christian Koeberl, and Mark Pilkington on earlier versions of the manuscript significantly improved its quality. This research was supported by grants from the National Aeronautics and Space Administration Planetary Geology and Geophysics Program Office to the Jet Propulsion Laboratory, California Institute of Technology.

## REFERENCES CITED

Anderson, R. R., 1986a, Geology of the Precambrian surface of Iowa: Geological Survey Bureau, Open File Map 86-1.

Anderson, R. R., 1986b, Structural configuration of the Precambrian surface of Iowa: Geological Survey Bureau, open File Map 86-2, Iowa Department of Natural Resources, Iowa City.

Anderson, R. R., and Hartung, J., 1992, The Manson impact Structure: Its contribution to impact materials observed at the Cretaceous/Tertiary Boundary: *in*, Proceedings Twenty Second Lunar Planetary Science Conference, p. 101-110,

Anderson, R. R., Hartung, J., Shoemaker, E. M., and Roddy, D. J., 1992, Preliminary results of the U. S. Geological Survey - Iowa Department of Natural Resources, Geological Survey Bureau Manson core drilling project: Preprint, international Conference on large impacts.

Black, R. A., Anderson, R. R., Keiswetter, D., and Steeples, D. W., 1992, Structure of the Manson features, Iowa, interpreted from Vibroseis and high resolution (rifle source) seismic reflection surveys [abs.]: EOS (American Geophysical Union Transactions), v. xx, p. 354.

Coons, R. L., Wool lard, G. P., and Hershey, G., 1967, Structural significance and analysis of the mid-continent gravity high: American Association Petroleum Geologists Bulletin, v. 51, p. 2381-2399.

Dryden, J. E., 1955, A study of a wc]] core from crystalline rocks near Manson, Iowa: [MS Thesis], University of Iowa, 89 p.

Dyrelius, D., 1988, The gravity field of the Siljan ring structure: *in*, Deep Drilling Crystalline Bedrock, Volume 1, The Deep Gas Drilling in the Siljan impact Structure, Sweden and Astroblemes, [Boden, A., and Eriksson, K. G., (eds.)], p. 85-94,

Ernstson, K., and Pohl, J., 1974, Some comments on the geophysical logging measurements in the Nordlingen 1973 research bore hole: Geologica Bavarica, V. 72, p. 81-90.

French, B. M., 1984, Impact event at the Cretaceous - Tertiary Boundary: A possible site: Science, v. 226, p. 353.

Grieve, R. A. F., 1991, Terrestrial impact: The record in the rocks: Meteoritic, v. 26, p. 175-194.

Grieve, R. A. F., Robertson, P. B., and Dence, M. R., 1981, Constraints on the formation of ring impact structures, based on terrestrial data: *in*, Multi-Ring Basins, Proceedings of the Lunar and Planetary Science, vol. 12A, [Schultz, P. H., and Merrill, R. B., (eds.)], Pergamon, New York, p. 37-57.

Gupta, V. K., Grant, F. S., and Card, K. D., 1984, Chapter 18, Gravity and magnetic characteristics of the Sudbury structure, *in*, The Geology and Ore Deposits of the Sudbury Structure: [I'ye, E. G., Naldrett, A. J., and Giblin, P. E. (eds.)], Ontario Geological Survey, Special Volume 1, p. 381-410.

Hartung, J. B., and Anderson, R. R., 1988, A compilation of information and data on the Manson impact Structure: Lunar and Planetary Institute Technical Report 88-08, 32 p.

Henderson, J. R., and Vargo, J. L., 1968, Aeromagnetic map of central Iowa: U. S. Geological Survey Geophysical Investigations Map GP-476.

Hershey, H. G., 1969, Geologic map of Iowa: Iowa Department Natural Resources, Geological Survey Bureau, Iowa City.

Holtzman, A. F., 1970, Gravity study of the Manson "Disturbed Area," Calhoun, Pocahontas, Humboldt, and Webster Counties, Iowa: [Master's Thesis], The University of Iowa, Iowa City, 63 p.

Hoppin, R. A., and Dryden, J. E., 1958, An unusual occurrence of Pre-Cambrian crystalline rocks beneath glacial drift near Manson, Iowa: Journal Geology, v. 66, p. 694-699.

Izett, G. A., Cobban W. A., Obradovich, J. D., and Kunk, M. J., 1993, The Manson impact Structure:  $^{40}\text{Ar}/^{39}\text{Ar}$  age and its distal impact ejects in the Pierre Shale in southeastern South Dakota, Science, v. 262, p. 729-732.

Izett, G. A., Reynolds, R. I., Rosenbaum, J. G., and Nishi, J. M., 1993, A Discontinuous melt sheet in the Manson impact Structure [abs.]: Abstracts Twenty-fourth Lunar and Planetary Science Conference, p. 705-706.

Munter, J. A., Ludvigson, G. A., and Bunker, B. J., 1983, Hydrogeology and stratigraphy of the Dakota formation in northwest Iowa, Iowa (geological Survey, Water Supply Bulletin 13, p. 1-55).

Norton, W. H., 1928, Deep wells of Iowa: Iowa Geological Survey, v. 33, 246-254.

Norton, W. H., and others, 1912, Underground water resources of Iowa: Iowa Geological Survey, v. 21, p. 29-118.

Pilkington, M., and Grieve, R. A. F., 1992, The geophysical signature of terrestrial impact craters: Reviews of Geophysics, v. 30, p. 161-181.

Sharpton, V. I., and Grieve, R. A. F., 1990, Meteorite impact, cryptoexplosion, shock metamorphism: A perspective on the evidence at the K/T boundary, *in* Global catastrophes in Earth history: An interdisciplinary conference on impacts, volcanism, and mass mortality [Sharpton, V. I., and Ward, P. D. (eds.)], Geological Society of America, Special Paper 247, p. 301-318.

Shoemaker, E. M., Roddy, D. J., and Anderson, R. R., 1993, Research program on the Manson Impact Structure, Iowa [abs.]: Abstracts Twenty-fourth Lunar and Planetary Science Conference, p. 1301-1302.

Smith, "T. A., 1971, A seismic refraction investigation of the Manson disturbed area: [Masters Thesis], University Iowa, 64 p.

Thiel "T. (. , 1956, Correlation of gravity anomalies with the Keweenaw geology of Wisconsin and Minnesota: Geological Society of America Bulletin, v. 67, p. 1079-1100.

U. S. Geological Survey, 1976, Aeromagnetic map of Iowa: U.S. Geological Survey Geophysical Investigations Map GP-910.

Zietz, I., Gilbert, F., and Kirby, J., 1976, Aeromagnetic map of Iowa: Color coded intensities: U. S. Geological Survey Geophysical investigations Map GP-911.

## FIGURE CAPTIONS

Figure 1. Map showing the location of the Manson impact structure in northwest Iowa. The 36 km diameter of the structure is indicated by the circle with a dot at the center.

Figure 2a. Bedrock geology map of the region surrounding the Manson impact structure from Hartung and Anderson (1988), modified from Hershey (1969) and Munter and others (1983). In stratigraphic order: Ku: Manson Disturbed Area; Kc: Carlile Shale; Kgl: Greenhorn limestone; Kgs: Graneros Shale; Kdw: Woodbury Member - Dakota Formation; Kdn: Nishnabotna Member - Dakota Formation; Jfd: Fort Dodge Beds; Pch: Cherokee Group; Mm: Meramec Series; Mk: Kinderhook Series; Du: Devonian Undifferentiated; Om: Maquoketa Formation; Og: Galena Group; PCC: Proterozoic Undifferentiated. 2b. Geologic sketch map of the Precambrian surface in the Manson area (from Hartung and Anderson 1988). Mkc: Keweenawan elastic rocks; Mkt: Keweenawan volcanic rocks; Mp: plutonic rocks; Ip: Penokean rocks.

Figure 3. Locations of gravity stations used in this study. Data points include those of Holtzman (1970) and those collected during this study. Shaded circle indicates position and diameter of the Manson structure.

Figure 4. (a) Simple Bouguer gravity map of the Manson region, Data are contoured with a 2 mGal contour interval after being gridded using a 50 x 50 element grid. "A" denotes the location of the central uplift. "." indicates station locations in all figures, (b) 3-D representation of the simple Bouguer gravity field, viewed from the south,

Figure 5a, Contour map of the 5th-order polynomial surface with a contour interval of 0.5 mGal, 5b. 3-D representation of the 5th order polynomial surface viewed from the south, This surface is assumed to represent the regional gravity.

Figure 6a. Contour map of the 5th-order residual gravity for Manson impact. Shaded areas have gravity > 1mGal; striped areas have gravity < -2mGal. Central stippled region indicates shallow Proterozoic crystalline rock (the central peak). Dashed line denotes boundary between moat and ring graben zones; solid outer line marks the inferred edge of the structure. Letters refer to locations discussed in text. 6b. 3-D representation of the 5th-order residual gravity as viewed from the south.

Figure 7. East-West seismic reflection profile across the Manson structure (from Anderson and Hartung, 1992). Also shown is the simple Bouguer gravity (in light dashed lined) and residual gravity (in dark line) for the profile,

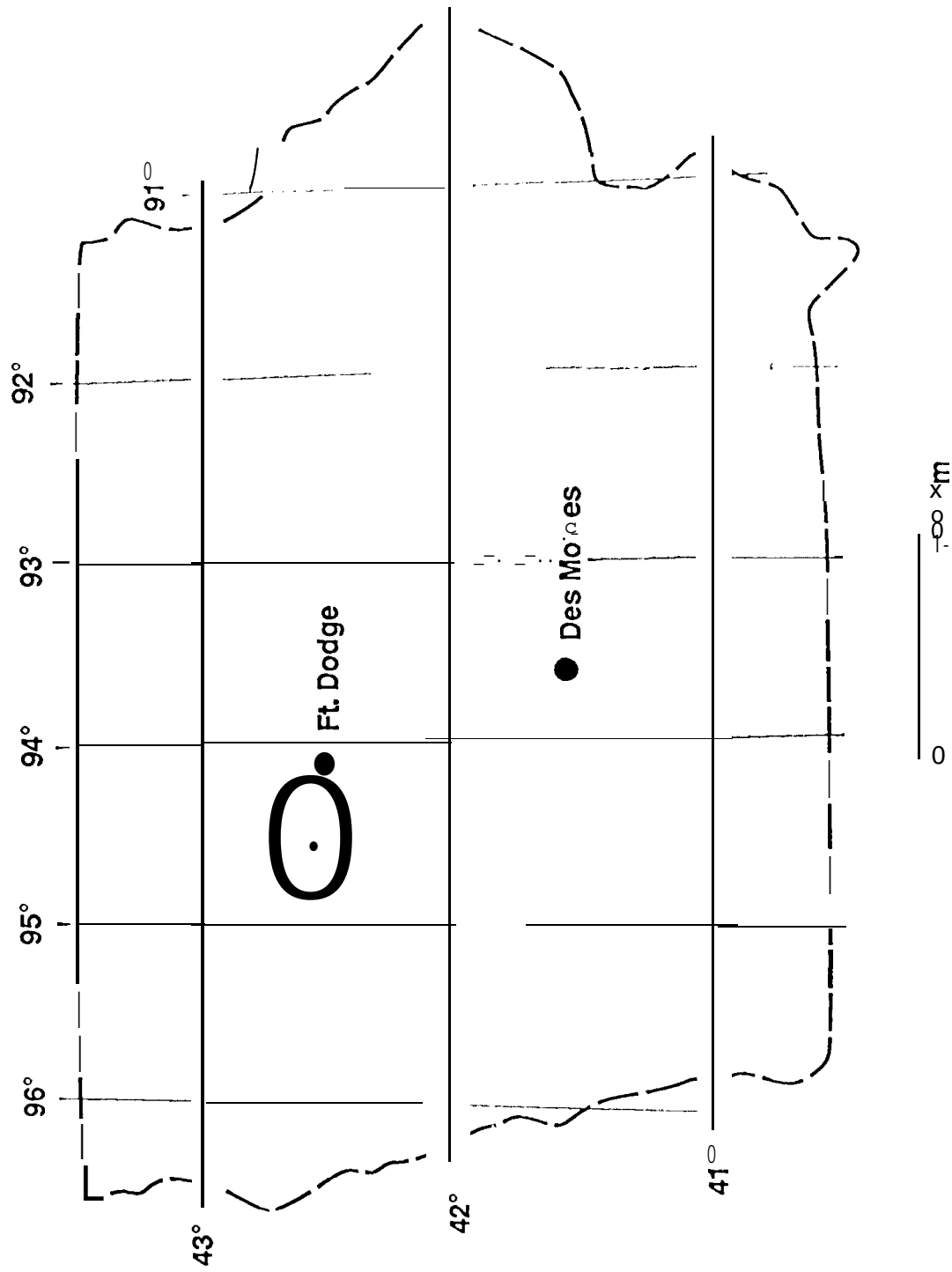


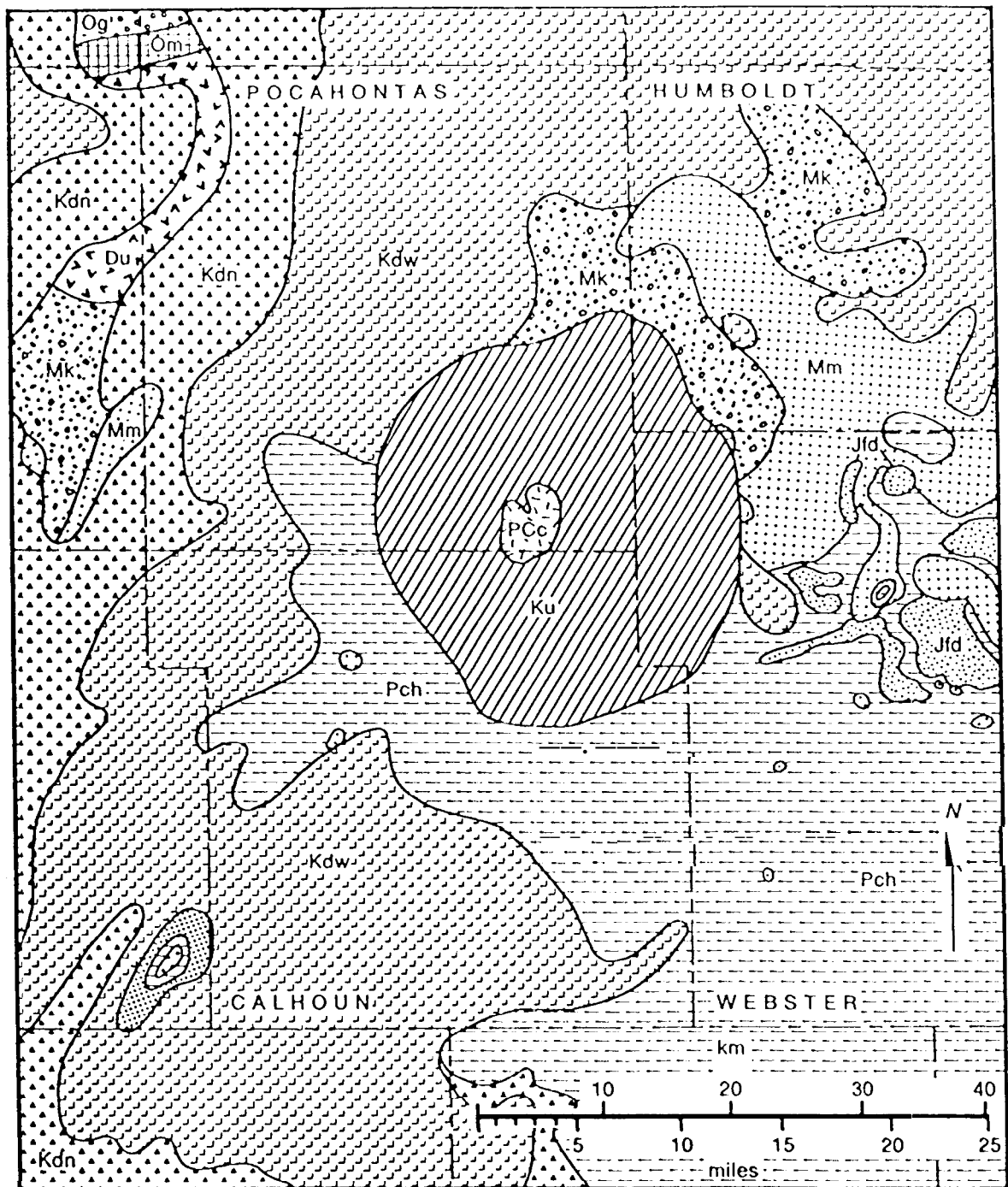
Figure 8. Density determinations for material from the M 1 core. (+ ) indicates Suevite; (O ) indicates impact melt breccia, (A ) indicates fragmental breccia. Depths are in meters below the surface.

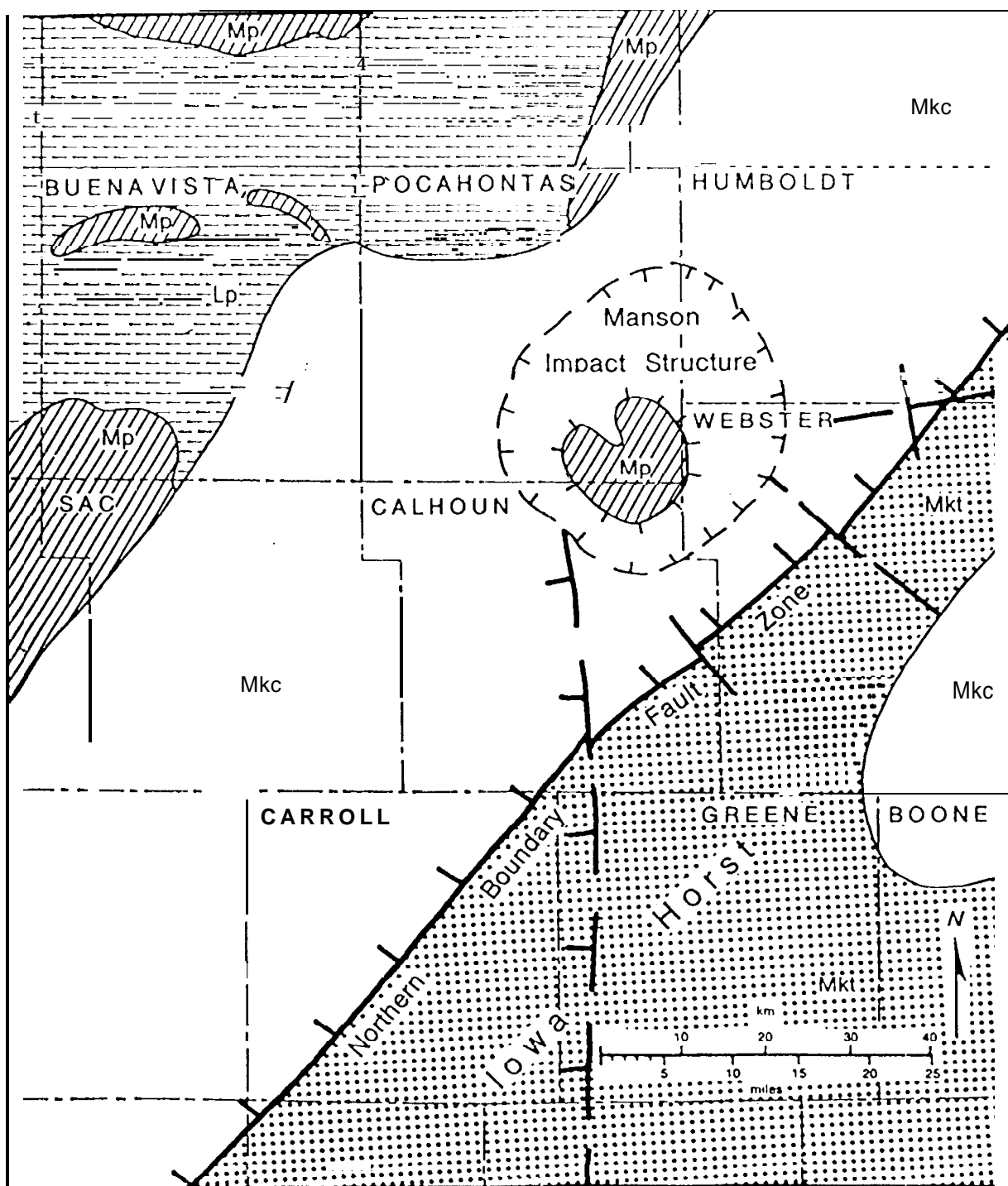
Figure 9. Gravity model of the radial structure of the Manson impact along the reflection profile. Patterns indicate different major lithologies; basement complex, impact breccia, Red Clastics, Paleozoic section, Tertiary sediments, and glacial till. Numbers indicate model body numbers; numbers in parentheses are densities in  $\text{g cm}^{-3}$ .

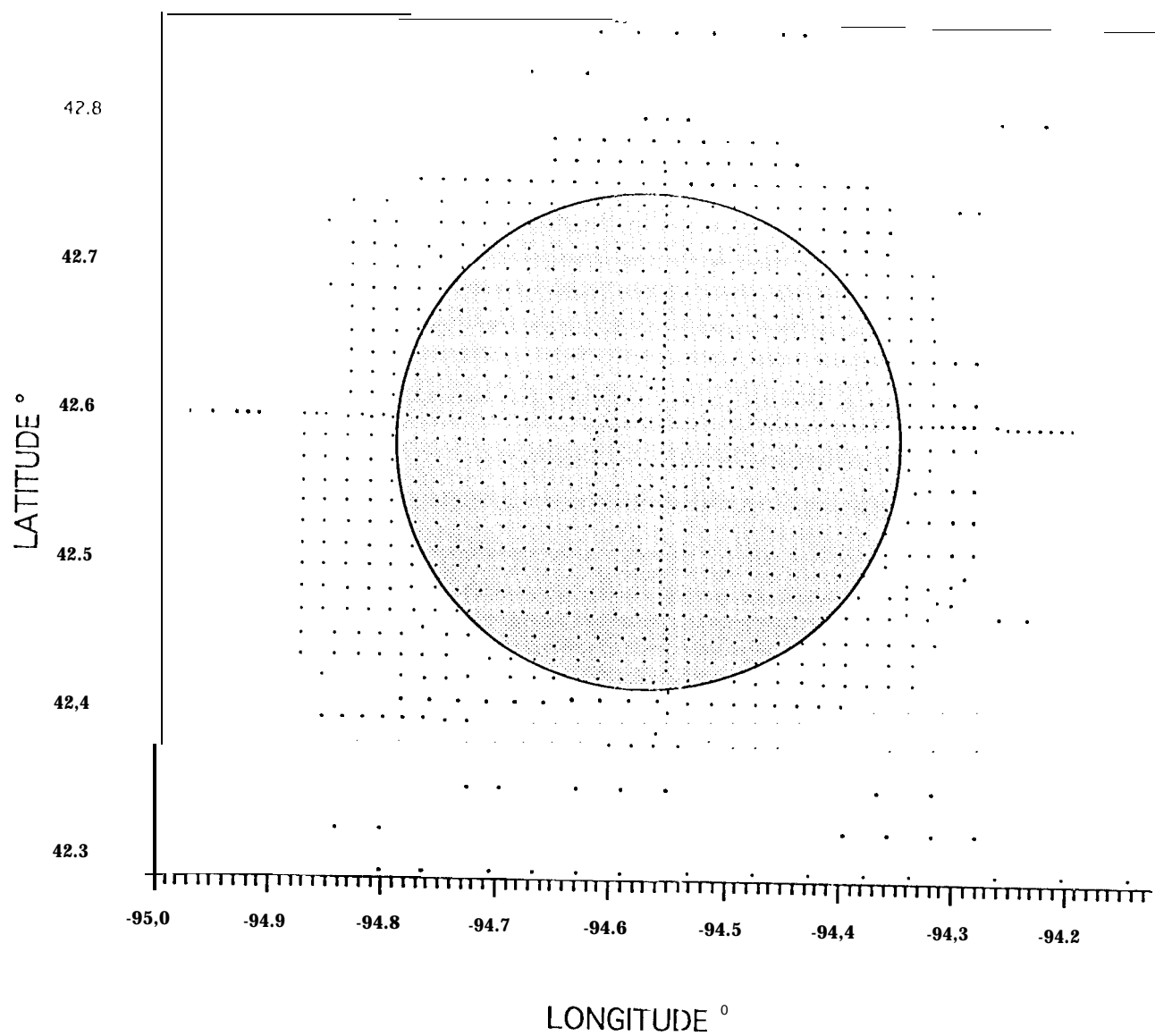
Figure 10. Total aeromagnetic field map of the Manson region between  $42^{\circ}$ - $43^{\circ}$  N and  $94$ - $95^{\circ}$  (from U. S. Geological Survey, 1976), The circle denotes the location and diameter of the Manson structure. Contour interval is 100 nT.

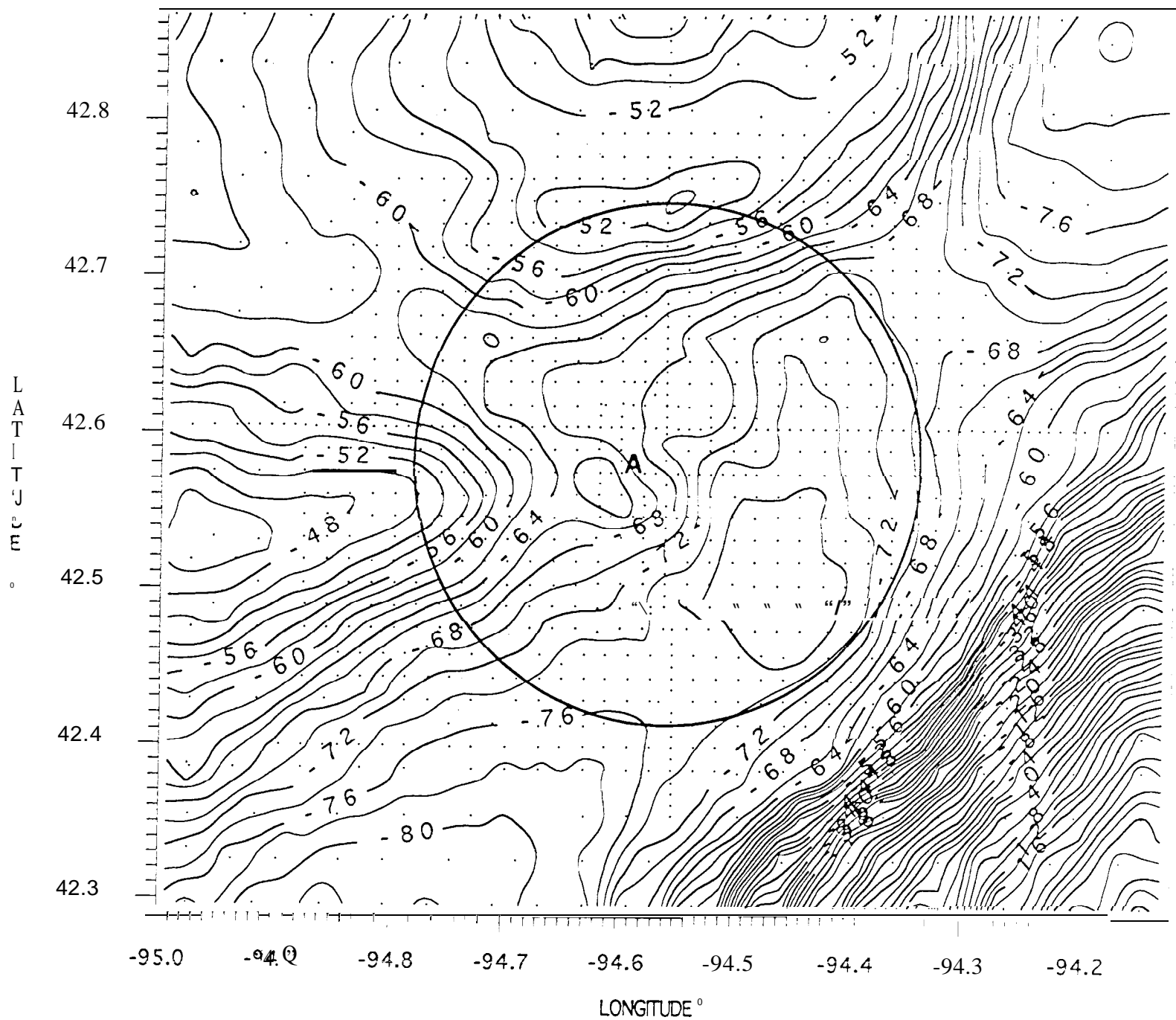
Figure 11. Maximum negative gravity anomalies for terrestrial impact craters (data from Pilkington and Grieve, 1992). The gravity anomaly for the Manson structure is indicated by the open circle.

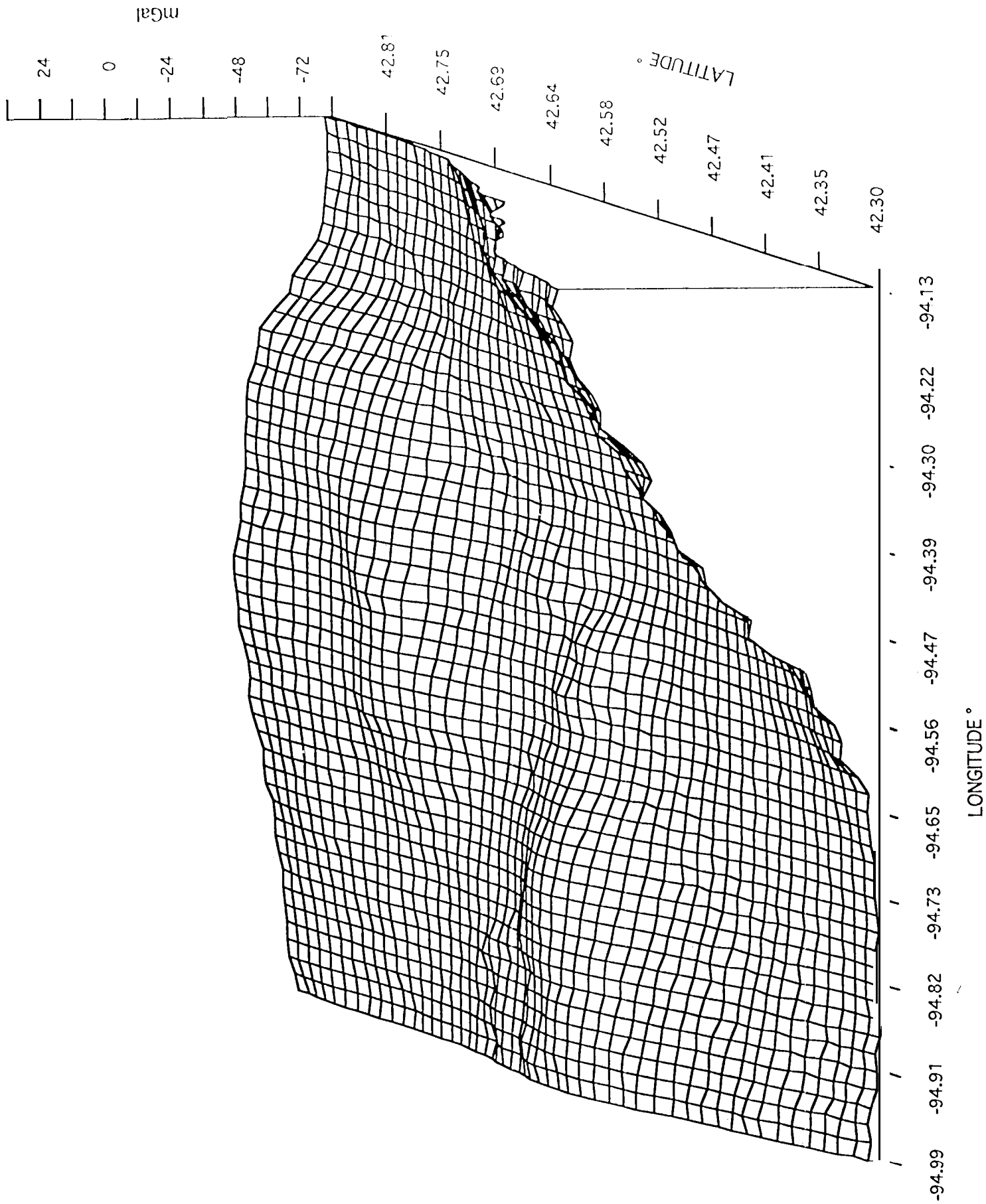


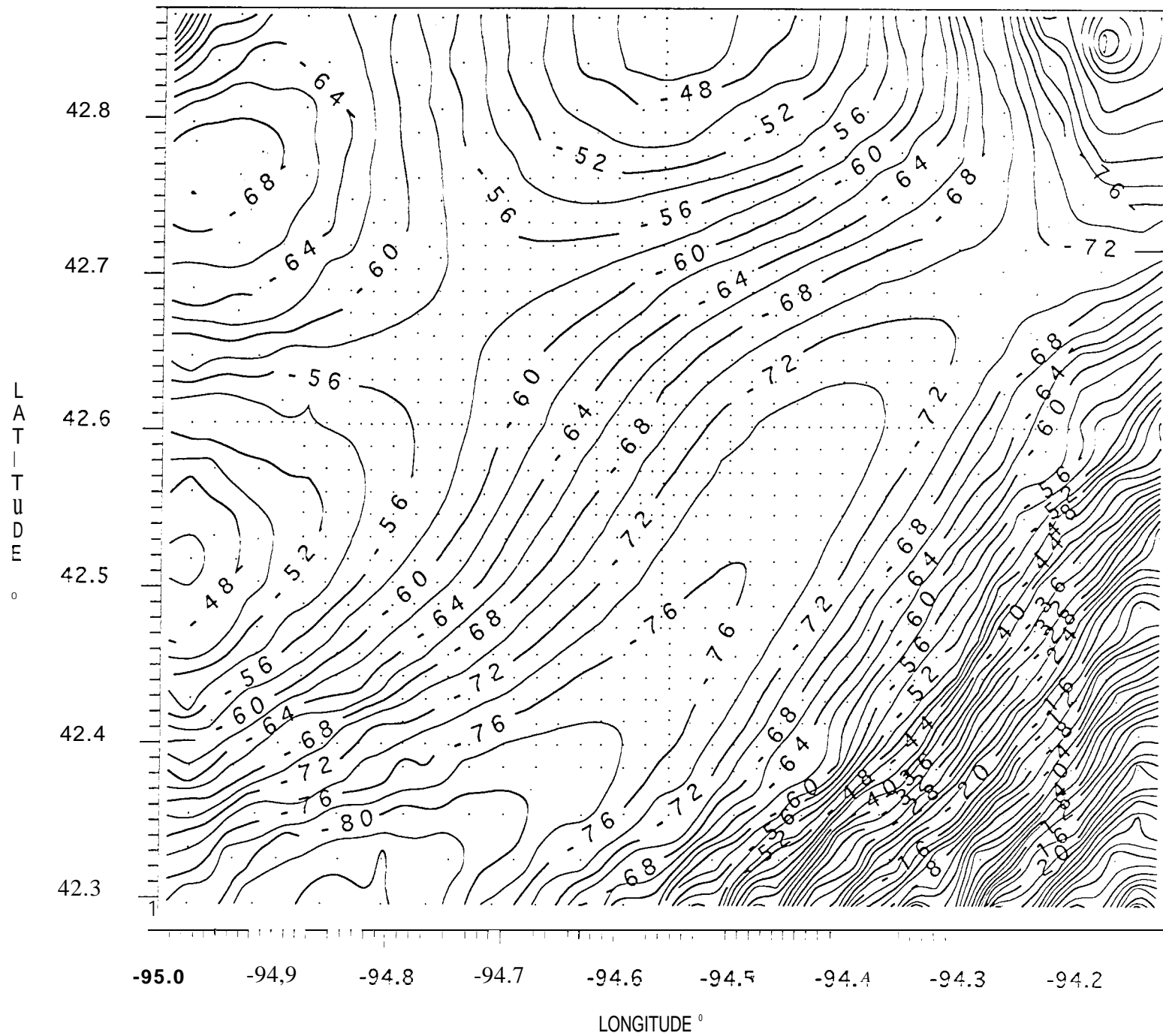




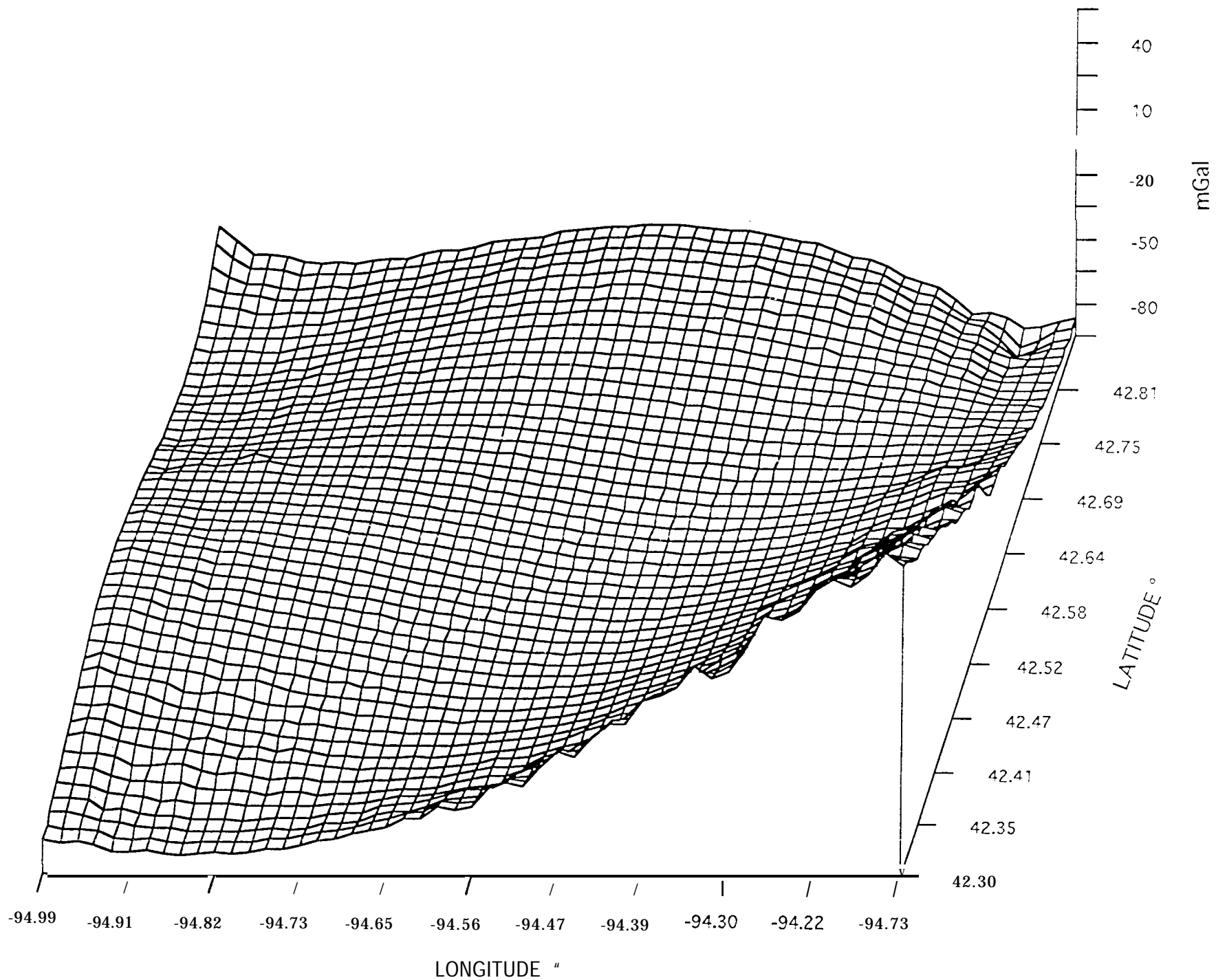


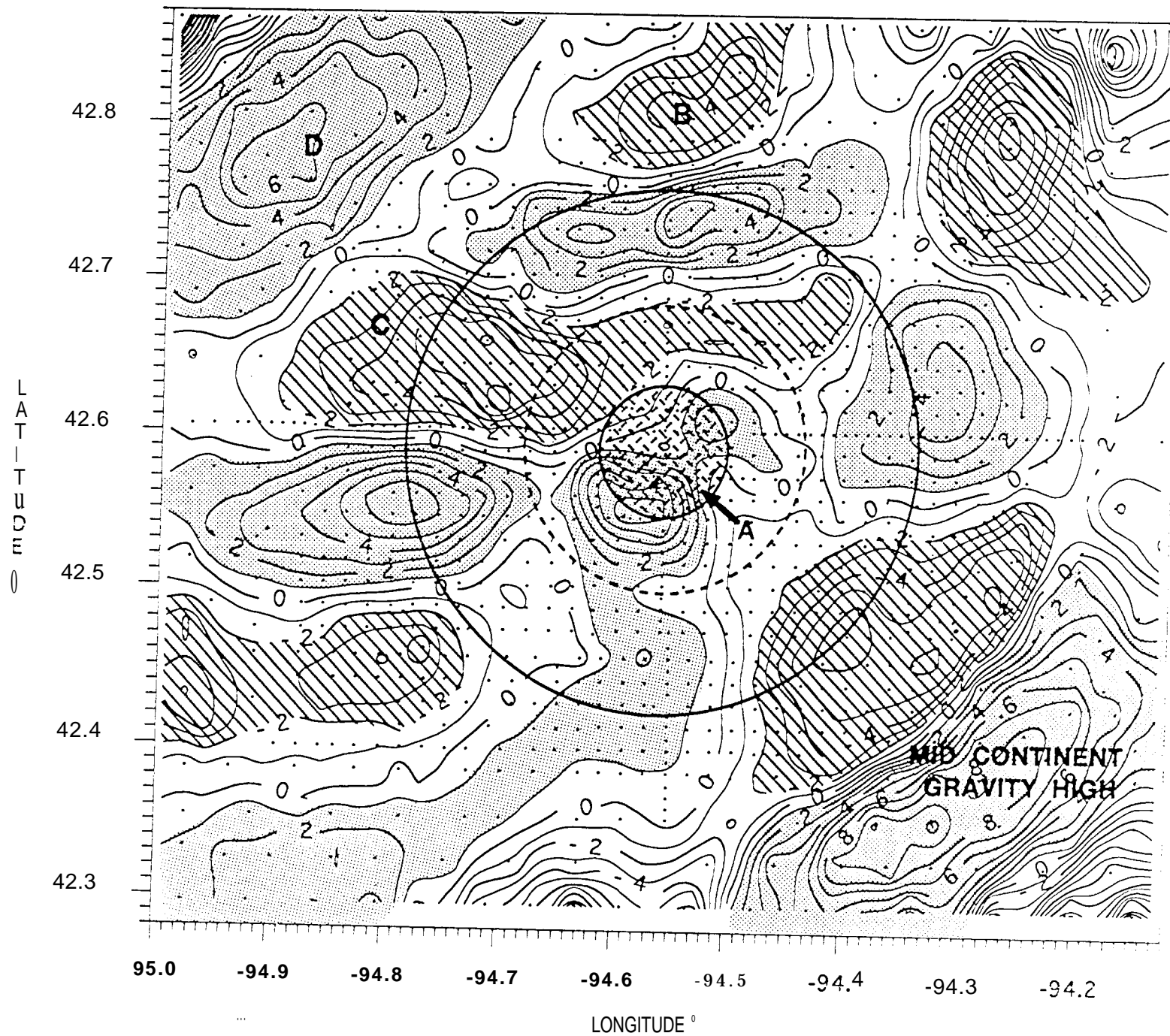


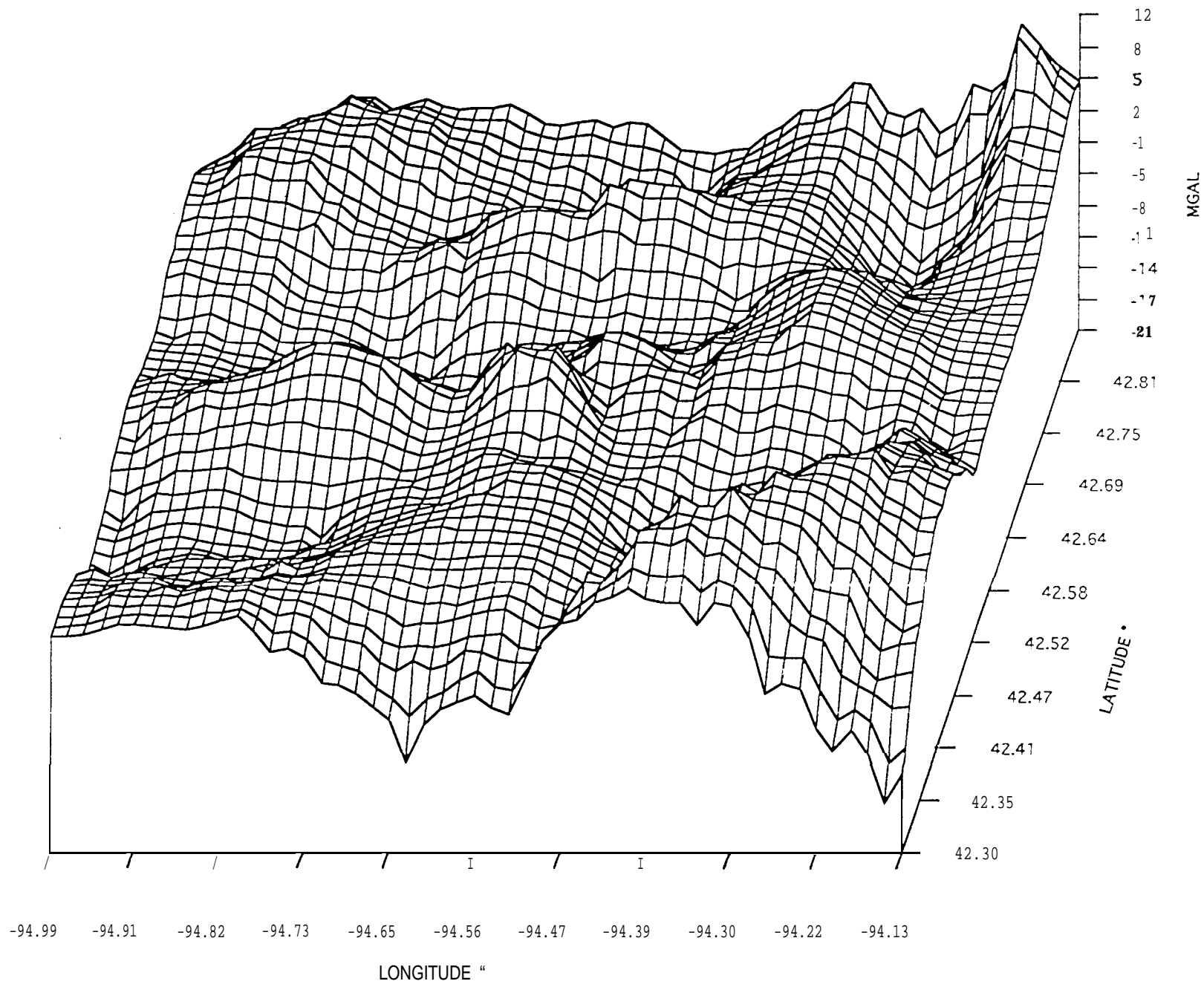


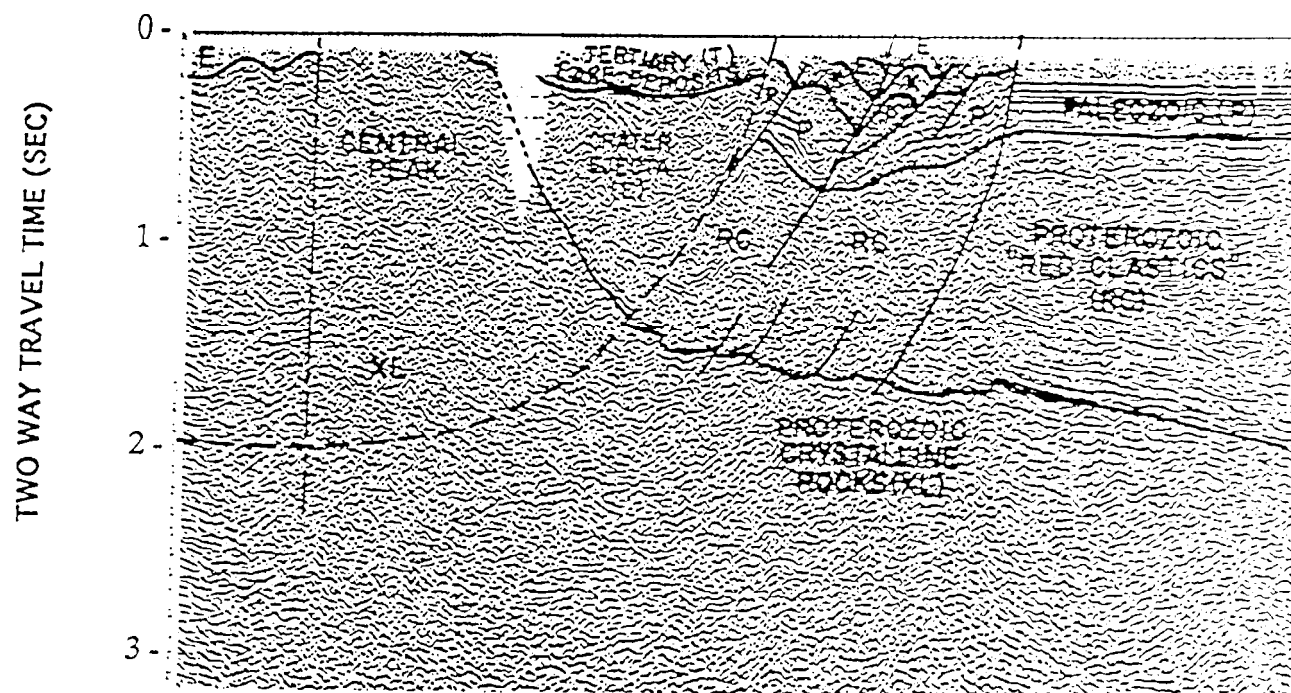
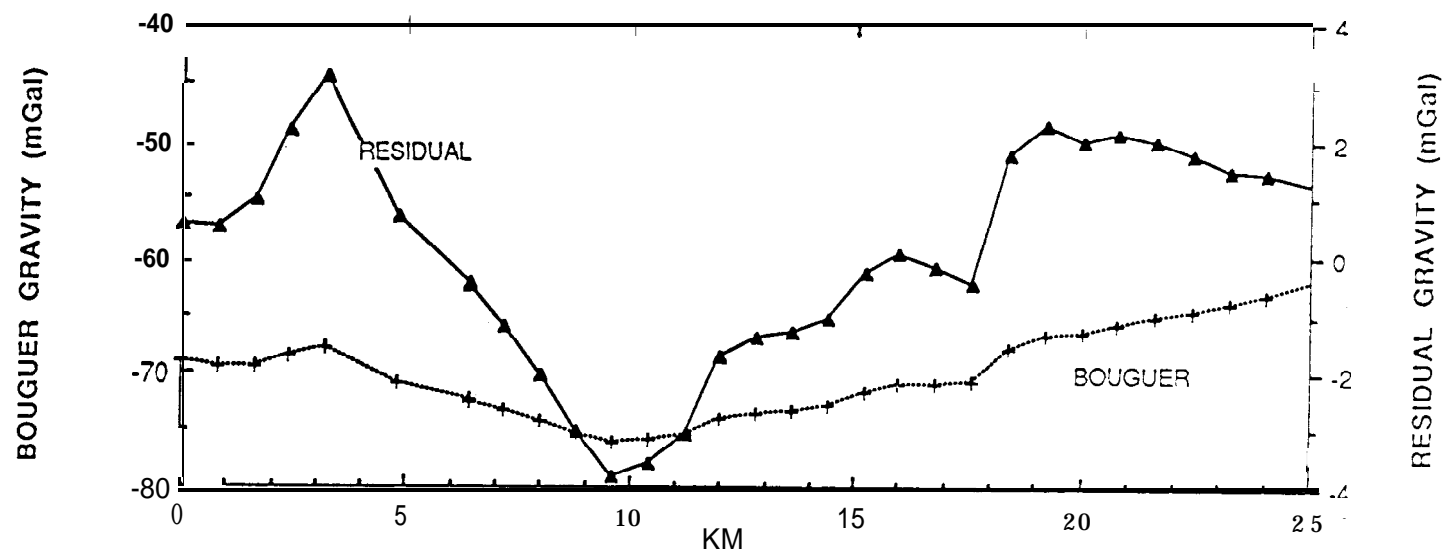


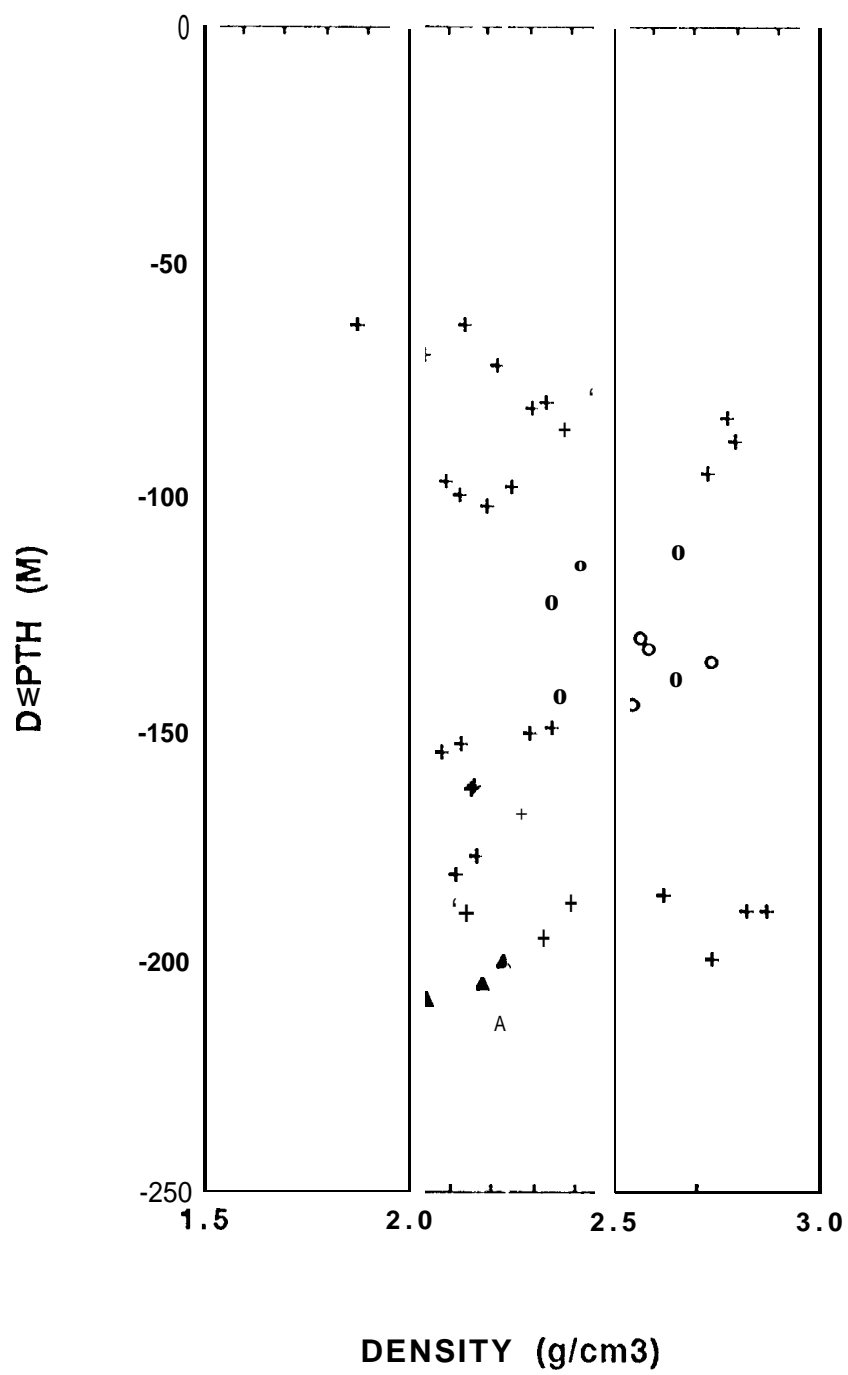


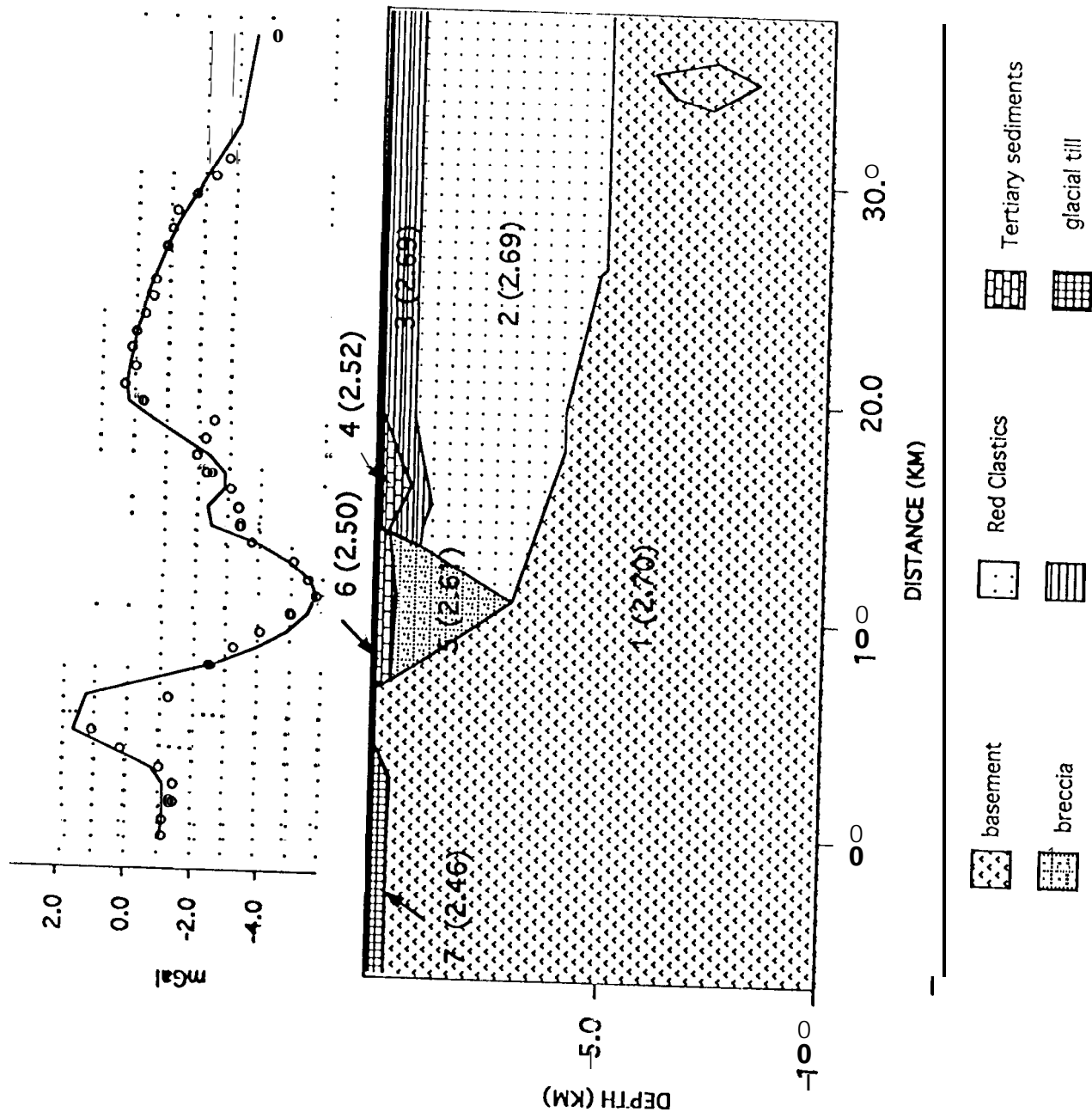


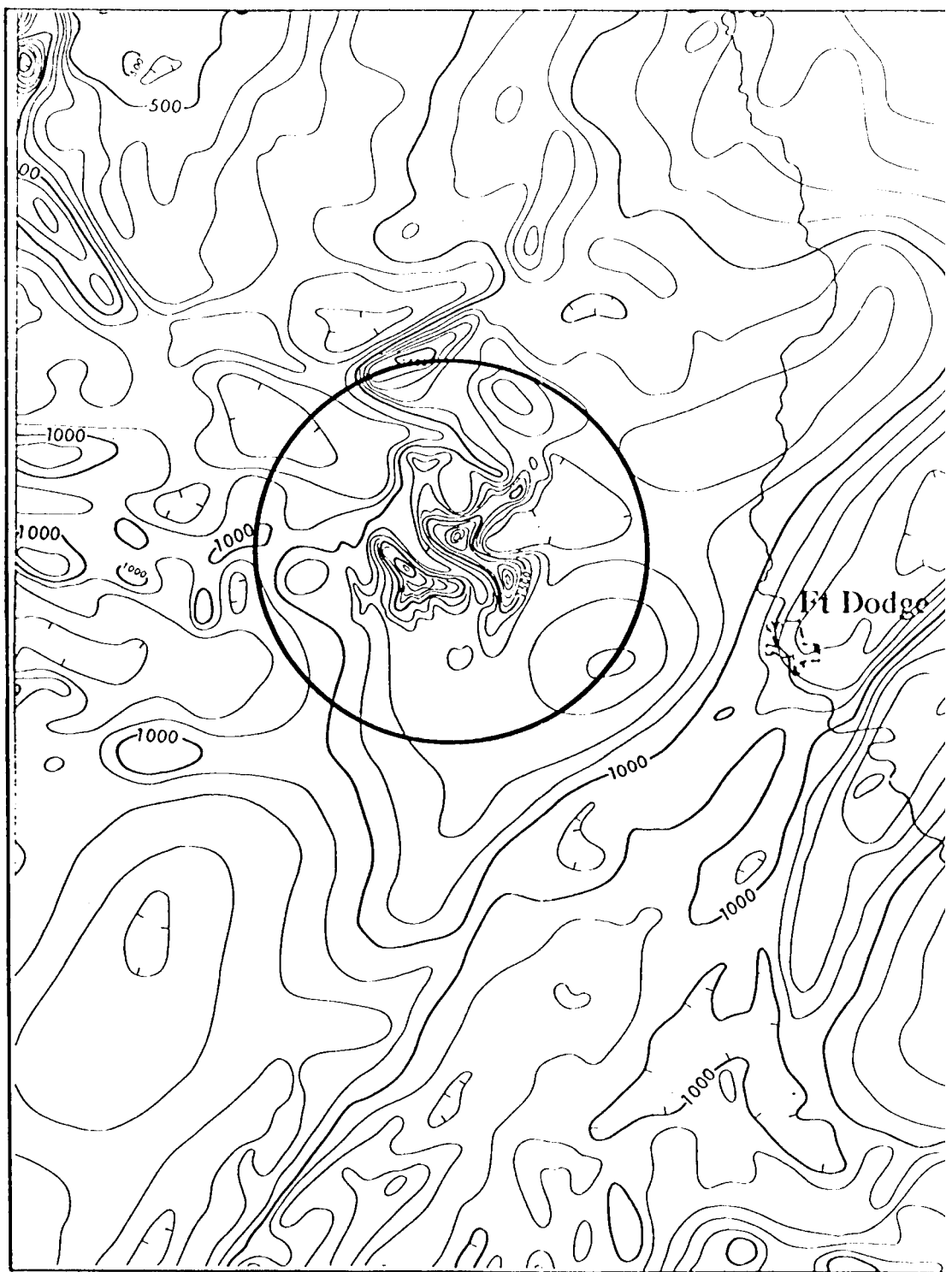












43"

0  
W  
TITUD  
S

42°

95°

LONGITUDE °

94°

